Climatic Change
DOI 10.1007/s10584-012-0493-6

Selected topics in arctic atmosphere and climate

William Perrie · Zhenxia Long · Hayley Hung · Amanda Cole · Alexandra Steffen · Ashu Dastoor · Dorothy Durnford · Jianmin Ma · Jan W. Bottenheim · Stoyka Netcheva · Ralf Staebler · James R. Drummond · N. T. O'Neill

Received: 30 January 2012 / Accepted: 7 May 2012
© Her Majesty the Queen in Right of Canada 2012

Abstract This paper summarizes the main elements of four IPY projects that examine the Arctic Atmosphere. All four projects focus on present conditions with a view to anticipating possible climate change. All four investigate the Arctic atmosphere, ocean, ice, and land interfacial surfaces. One project uses computer models to simulate the dynamics of the Arctic atmosphere, storms, and their interactions with the ocean and ice interface. Another project uses statistical methods to infer transports of pollutants as simulated in large-scale global atmospheric and oceanic models verifying results with available observations. A third project focuses on measurements of pollutants at the ice-ocean–atmosphere interface, with reference to model estimates. The fourth project is concerned with multiple, high accuracy measurements at Eureka in the Canadian Archipelago. While these projects are distinctly different, led by different teams and interdisciplinary collaborators, with different technical approaches and methodologies, and differing objectives, they all strive to understand the processes of the Arctic atmosphere and climate, and to lay the basis for projections of future changes. Key findings include:

- Decreased sea ice leads to more intense storms, higher winds, reduced surface albedo, increased surface air temperature, and enhanced vertical mixing in the upper ocean.

Electronic supplementary material The online version of this article (doi:10.1007/s10584-012-0493-6) contains supplementary material, which is available to authorized users.

W. Perrie (✉) · Z. Long
Fisheries and Oceans Canada, Bedford Institute of Oceanography, Dartmouth, Nova Scotia, Canada
e-mail: william.perrie@dfo-mpo.gc.ca

H. Hung · A. Cole · A. Steffen · J. Ma · J. W. Bottenheim · S. Netcheva · R. Staebler
Environment Canada, Air Qualtiy Research Division, 4905 Dufferin Street, Toronto, Ontario M3H 5T4, Canada

A. Dastoor · D. Durnford
Environment Canada, Air Qualtiy Research Division, 2121 TransCanada Highway, Dorval, Quebec H9P 1J3, Canada

J. R. Drummond
Department of Physics & Atmospheric Science, Dalhousie University, 6310 Coburg Road, Halifax, NS B3H1Z9, Canada

N. T. O'Neill
Département de géomatique appliquée, Université de Sherbrooke, Sherbrooke, Quebec, Canada

Published online: 02 August 2012

- Arctic warming may affect toxic chemicals by remobilizing persistent organic pollutants and augmenting mercury deposition/retention in the environment.
- Changes in sea ice can dramatically change processes in and at the ice surface related to ozone, mercury and bromine oxide and related chemical/physical properties.
- Structure and properties of the Arctic atmospheric—troposphere to stratosphere—and tracking of transport of pollution and smoke plumes from mid-latitudes to the poles.

1 Introduction

Observed and anticipated changes in Arctic atmosphere, climate, sea surface temperatures, sea ice, and storms contribute to increased risks to northerners and their communities (Zhang et al. 2004; Johannessen et al. 2004; IPCC 2007; ACIA 2004; Serreze et al. 2007). Large expanses of open water can create large waves and high risk of storm surge, resulting in coastal flooding and erosion. Higher temperatures thaw permafrost, resulting in coastline destabilization (Solomon 1994). Integrated studies of the Arctic atmosphere, climate, storms, and the ocean-ice interface are needed to clarify the impacts of climate change (Brunner et al. 2004; Serreze et al. 2007).

This paper presents a review of the principal components of four different Canadian IPY projects that investigate the Arctic atmosphere and climate. All four investigate the atmosphere within the context of the associated Arctic Ocean, ice, and land interfacial surfaces, and all are motivated by concerns related to climate change. In addition to trying to understand the present Arctic atmospheric state and its dynamics, the four projects try to understand the processes of, and potential for, change. However, the four projects are also distinctly different, performed by different teams, using very different technical approaches and methodologies, with differing objectives.

The first project, Impacts of Severe Arctic Storms (ImSAS), focused on coastal ocean processes, connecting storms, climate change, sea ice, and upper ocean conditions, and the coastal marine environment. This was a modeling project collaborating with field experiments funded by other initiatives. Here, studies of two Arctic summer storms are described, one with relatively extensive ice cover, and another, with minimal ice cover.

The second project was Intercontinental Atmospheric Transport of Anthropogenic Pollutants to the Arctic (INCATPA), focusing on the northward movement of persistent organic pollutants (POPs) and mercury (Hg), toxic chemicals that can be carried by atmospheric or oceanic circulations to the Arctic. One component of this project used statistical techniques to detect climate change impacts in observed atmospheric concentration data; this will provide information for future estimations of changes on the distribution of these pollutants in the Arctic.

The third project was Ocean Atmosphere Sea Ice and Snow Interactions in polar regions (OASIS—Canada), focusing on measurements and understanding of lower atmosphere chemistry over the Arctic Ocean surface, as driven by processes in the atmosphere and at the ice-ocean–atmosphere interface. OASIS investigated the properties and possible changes (e.g. weather and climate related) of O_3, mercury, and bromine monoxide (BrO). In situ and remotely sensed data are being acquired in order to verify and extend these results.

The fourth project is the Polar Environment Atmospheric Research Laboratory (PEARL), located at Eureka in Nunavut. Through PEARL it was possible to make year-round atmospheric measurements, to better inform whole-year and whole-atmosphere studies of the High Arctic with more accurate estimates of composition, including ozone and related gases, polar winter aerosols and spring aerosols, and tracking the spread of smoke and pollution from the lower part of the atmosphere to the upper part, where they can affect weather and climate.

2 Impacts of Severe Arctic Storms and climate change on the coastal ocean (ImSAS)

Storms can modify the transport of heat, moisture and contaminants between the Arctic and lower latitudes, and their dynamics occupy the atmospheric column from the ocean-ice surface to the top of the troposphere. While storms may be driven by upper level atmospheric processes, their development, intensities and tracks are modulated by air-sea fluxes and the sea ice distribution, which they influence through storm-generated waves, currents and winds. Thus, Arctic cyclones and their role in atmospheric dynamics and climate constitute a potential link to the other three IPY projects considered in this paper. The importance of understanding these dynamics is further enhanced in the context of changing climate, in particular the significant decline in sea ice cover. Simmonds and Keay (2009; see also Simmonds et al. 2008) suggest that there is a trend for Arctic cyclones to have increasing size and intensity, with no detectable change in frequency.

The ImSAS IPY project focused on severe Arctic storms, with central sea level pressure (SLP) less than 980 hPa, and their impact on the upper ocean and coastal zone. Changing climate has led to declining sea ice cover and large open water areas, with changes in ocean surface fluxes. In turn, these influence the Arctic storm climate and have impact on the upper ocean and sea ice. These effects are largest in the summer and autumn due to the combined intense cyclonic activity occurring at that time, sea ice retreat, and the greater availability of enhanced heat and moisture fluxes from the open-water portion of the ocean.

To represent differences in sea ice and climate scenarios, two moderately strong cyclones are considered: one in 1999 when the open water was relatively modest, and the other in 2008, when a large area of open water was available. Together, they serve to increase our understanding of the effect of the ocean surface on intense Arctic cyclones.

2.1 1999 summer storm

On 21 September 1999 a cyclone (hereafter, the 1999 storm), originated over the Northeast Pacific, intensified explosively in the Gulf of Alaska, developed into a meteorological bomb, and made landfall with surface winds in excess of 25 ms^{-1} at Cape Newenham, Alaska, on 23 September. Moving to the north-northeast, it crossed the Rocky Mountains and re-intensified over coastal waters of the southern Beaufort Sea, between the coast and pack ice, creating a storm surge and coastal flooding with extensive ecological damage, unmatched in the past 1,000 years (Pisaric et al. 2011). It then moved northeastward, dissipating over the Canadian Archipelago by 26 September.

The 1999 storm is notable because of its storm surge. During this storm, winds ranged from southeasterly on 22 September, ahead of the storm, to northwesterly on 26 September, behind the storm on the southern Beaufort coast. In an analysis of data from a field experiment by S. Solomon, funded by collaborating projects, Mulligan et al. (2010), considered a similar wind event in August 2007. They used in situ and remotely sensed data (see Supplementary File #1, Figure S1) to investigate the nearshore Mackenzie Delta water levels and currents and their rapid response to local winds. Southeasterly winds give negative surge, or set-down, whereas northwesterly winds give positive surge, or set-up. During the 1999 storm, during the negative surge (set-down), relatively fresh water left the nearshore areas; as the storm passed northwesterly, winds created a positive surge with higher salinity, flooding coastal areas, and killing vegetation as far as 30 km inland (Pisaric et al. 2011; Melling et al. 2011, *this issue*; see also Supplementary File #2).

Such severe impacts beg the question: what are the climatological precursors that tend to generate storm surges? Small et al. (2011) note that storm surge in the Mackenzie Delta

region tends to occur during persistent northwesterly winds in the late summer when sea ice is minimal. They suggest that if conditions favor strong northwesterly geostrophic winds with relatively low static stability, then strong persistent northwesterly winds are possible at the surface, associated with an anomalously low pressure centre northeast of the Mackenzie Delta and a high pressure centre over the Bering Sea and eastern Siberia; storm surges can occur. Analysis of the 1999 storm, by Small et al. (2011), show that winds at the Delta were from the northwest on September 23. At the same time, an anticyclone located along the Beaufort coast of west Alaska, created a deformation zone over the Beaufort Sea, with a confluence zone between the cyclone-anticyclone dipole over the Chukchi with strong northerly surface winds. From the 950 hPa potential temperature field, Small et al. suggest the formation of an area of cold air north of the mountains, and U-shaped ridging of SLP, creating a tight pressure gradient and strong northwesterly geostrophic winds along the Beaufort coast. As the cyclone moved eastward, followed by the cold air pool that followed the coastal topography, the SLP increased along the northern edge of the topography, causing the pressure gradient to increase to the north, and the surface northwesterlies to strengthen.

Two experiments were conducted using a coupled atmosphere-ice-ocean model to explore the interactions between the storm, the ocean and the ice, and the role of surface fluxes on the storm's life cycle. In the "coupled" experiment, the coupling processes were enabled, whereas in the "uncoupled" experiment, the coupling processes were disabled. The coupled model system consisted of a modern mesoscale atmospheric model and an ice-ocean model (Perrie et al. 2004; Long et al. 2011). SSTs, ice concentration and thickness are passed from the ocean surface to the atmospheric model, while surface air temperature, winds, SLP, clouds, precipitation and specific humidity from the atmospheric model are passed to the coupled ice-ocean model, at each coupling time step. For the atmospheric part, a relatively high horizontal resolution was used (30 km, 30 vertical layers, 25 min time steps), taking initial and boundary conditions from Canadian Meteorological Centre analyses. The ice-ocean part used 23 vertical sigma levels with higher resolution in the upper mixed layer, lower resolution in the deep ocean, and ~27 km horizontal resolution (Mellor and Kantha 1989; Hibler 1980). Polar Science Center Hydrographic Climatology data are used for initial and boundary conditions (Steele et al. 2001), with prescribed inflow/outflow conditions at Bering Strait, Canadian Archipelago, Norwegian Sea and along Greenland's east coast (Long et al. 2011). The ice-ocean part was spun-up for 7 years using NCEP monthly reanalysis data, and another 14 years to 1999 with daily NCEP reanalysis data. In "uncoupled" simulations, feedbacks from the ice-ocean surface are not passed back to the atmosphere.

Model results indicate that the 1999 storm coincided with an initially warm, shallow (thin) oceanic mixed layer in the southern Beaufort Sea, overlying cold Arctic waters. Feedbacks from the ocean surface to the storm were enhanced by the thin oceanic mixed layer, slow storm propagation speed, and strong thermal stratification below the mixed layer. Although the extent of the open water is relatively modest (Fig. 1), a weak cool SST wake did form and surface heat fluxes resulted in slight reductions to storm intensity (Fig. 2) consistent with studies of tropical storms (Schade and Emanuel 1999). The influence of relatively strong winds (>20 $m \cdot s^{-1}$) distributed the cool SST wake widely along Beaufort coastal areas. This was accentuated when the storm's propagation slowed and it lingered over the southern Beaufort, as near-surface winds dramatically intensified. Maximum SST cooling (~1.5°C) involved entrainment of cooler water from beneath the mixed layer, and mixing related to strong vertical shear. Ocean surface feedbacks weakened the storm, reducing winds by up to ~1 m/s (Fig. 2).

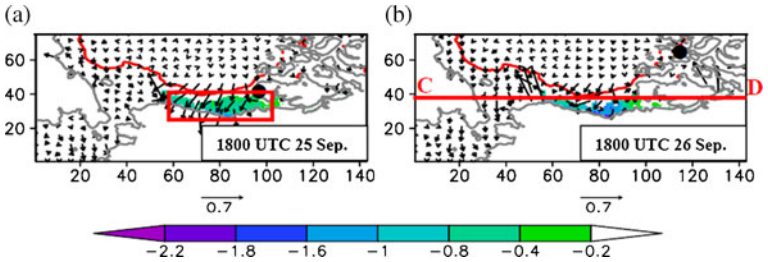

Fig. 1 Coupled model results for the storm-induced surface currents ($m\ s^{-1}$) and differences in the SST distributions (ºC) at (**a**) 72 h and (**b**) 96 h, minus the initial SST. The red contour gives the location of 0.15 ice concentration which provides an approximation to the ice edge. Black dot indicates the location of the storm. Cross section C–D is used in Figure 3. The red box in **a** indicates an open water area of the Beaufort Sea used for averaging calculations

The main ocean-ice-atmosphere feedbacks during the storm occur over open water, where SST cooling and ocean mixed layer currents are induced by winds (Fig. 1), extending to 15 m vertically, particularly in southern Beaufort waters (Figure S2). Related surface currents reached ~0.4 ms^{-1}, extending to ~100 skm in the cross-track direction. In addition to currents, storm winds can affect sea ice, the ice edge and ice distribution. In return, sea ice and the ice edge can modulate air-sea fluxes (heat, moisture, and momentum) from the ocean, thereby defining a baroclinic zone that can influence storm activity (Serreze et al.

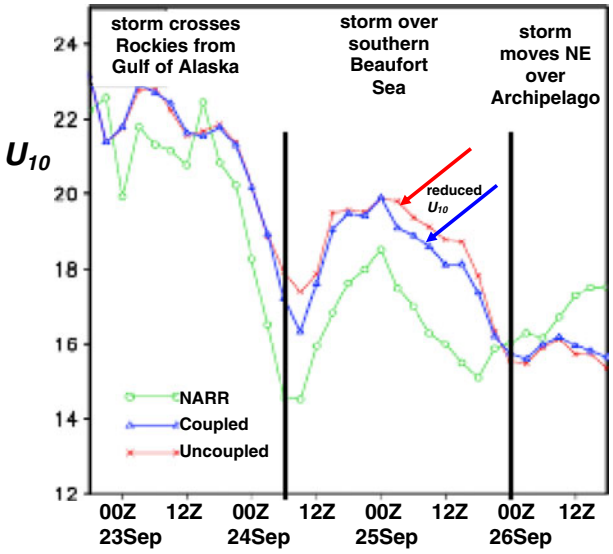

Fig. 2 Maximum U_{10} winds ($m\ s^{-1}$) from the Coupled (*blue white triangle*) and Uncoupled (red ×) model simulations, in comparison with NARR estimates. The 1999 storm re-intensified during its time over the southern Beaufort, from about 06Z on 24 Sep. until 00Z on 26 Sep., and the maximum values for U_{10} for the "Coupled" model system have smaller values than those of the "Uncoupled" model system. For coupled and uncoupled simulations, the time series of maximum U_{10} is calculated for each 3-hourly map, following the propagation of the central vortex-core of the storm. North American Regional Reanalysis (NARR) data is used for comparisons, which are high quality climate reanalysis data produced by the National Centers for Environmental Prediction (NCEP). U_{10} winds are marine winds corrected to standard 10 m reference elevation in neutral boundary layer conditions

2001; Simmonds et al. 2008). Thus, sea ice can retard storm progression into the Arctic by creating a cold friction zone where storms lose energy—over ice—whereas over southern Beaufort waters they can intensify.

Air-sea feedbacks during the 1999 storm cause the atmospheric boundary layer to become cooler and more stable, slightly de-intensifying the storm (Fig. 2), compared to scenarios where no feedbacks occur. Although the impacts on the maximum surface winds are small, they can cause reductions in sensible and latent heat fluxes, accompanied by cooling of the near-surface and lower atmosphere air temperatures. Reduced air-sea heat fluxes tend to cool and dry the atmospheric boundary layer, weakening the cyclone, resulting in decreases in surface winds.

Synoptic-scale processes drove the 1999 storm's baroclinic development, with the cooled ocean surface fluxes playing a secondary role, modifying the atmospheric boundary layer. When warm air moved over cold water, the atmospheric boundary layer stabilized because of negative sensible surface heat fluxes. Vertical mixing was suppressed as vertical wind shears increased, as surface drag decreased, and winds aloft increased. In contrast to the boundary layer, where ocean surface feedbacks and atmosphere–ocean coupling weakened, the cyclone became more intense in the mid-troposphere, with stronger winds surrounding the storm center.

2.2 2008 summer storm

The second example is a storm that occurred in the summer of 2008 (hereafter, the 2008 storm), when there was a large area of open water with a near record summer ice minimum. Thus the effect of air-sea fluxes was notable, influencing storm development. The storm originated in northern Siberia and slowly moved towards the Beaufort Sea. Intensifying from a relatively weak system over the Chukchi Sea, with minimum (SLP) of 990 hPa on 29 July, it reached its maximum intensity (minimum SLP, 976 hPa) the next day, as it slowly moved eastward near the ice edge (Fig. 3(i)). After lingering over open water over Canada Basin, it moved northeastward, slowly weakened and dissipated.

As with the 1999 storm, two experiments were performed with the atmosphere-ice-ocean model system. Here, the atmospheric portion of the coupled model system consisted of the Canadian Regional Climate Model (CRCM; see Caya and Laprise 1999; Laprise et al. 2003), because related studies look at climate change scenarios, and secondly, it is test for model-dependency in results from the two storms. CRCM is based on the same dynamical formulation as the mesoscale atmospheric model described in the previous section. In the "uncoupled" simulation, sea ice cover is prescribed by its climatology, and therefore the ocean does not respond with feedbacks to the atmosphere that evolve as the storm develops. In the "coupled" model system, the sea ice is predicted by the ice-ocean model, which is coupled to CRCM, and simulated air-sea feedbacks change as the storm grows and evolves. From climatology, the "uncoupled" simulation assumes ice cover over most of the Chukchi and Beaufort Seas, with only a narrow open-water region near the coast, as in past decades. The "coupled" simulation uses the ice-ocean model component to simulate the open water area, at the time of the 2008 storm.

In terms of minimum SLPs, results from the coupled and uncoupled simulations are similar, with differences within ~1 hPA of Canadian Meteorological Centre results (Fig. 3 (i)). For storm track, intensity, and observed ice edge, no large impacts of increased open water are initially evident. However, with respect to surface winds, the simulations do have significant differences. Figure 3(ii) compares results from coupled and uncoupled simulations to high-quality re-analysis winds, when the storm had intensified to its maximum

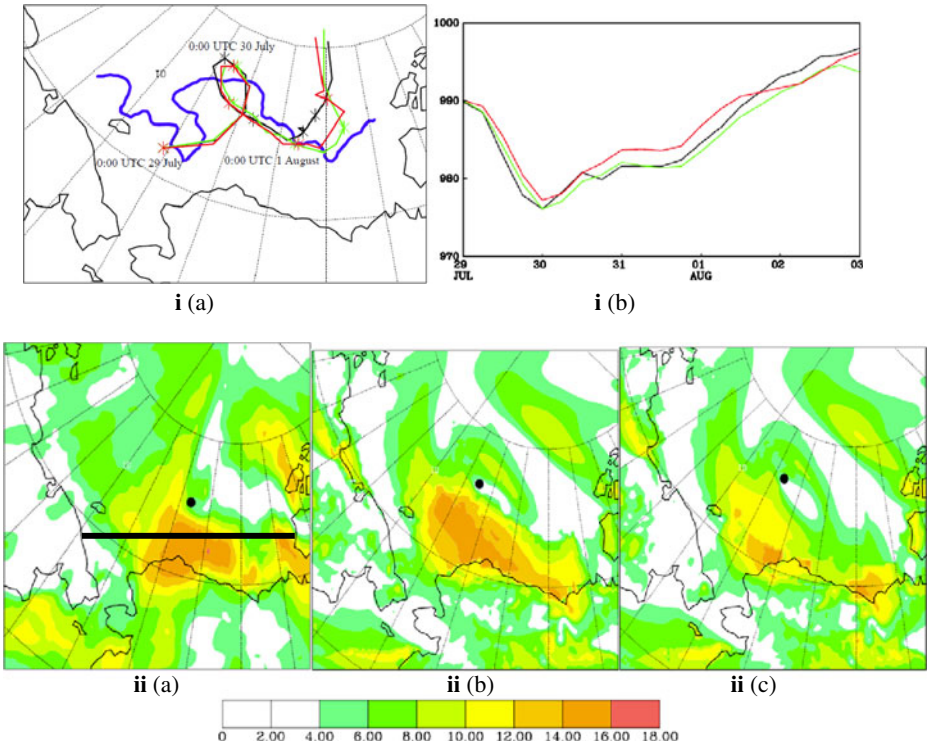

Fig. 3 **(i)** The July 2008 storm showing **(i) a** storm tracks and **(i) b** minimum central sea level pressure (SLP) following the storm trajectory, averaged over the (moving) area within 160 km of maximum wind, showing coupled model (green), uncoupled model (red), CMC (black) minimum SLP analyses. The thick blue line in **a** represents the US National Snow and Ice Data Center (NSIDC) ice edge. **(ii)** Maximum wind field distribution from **(ii) a** QSCAT-NCEP **(ii) b** coupled model **(ii) c** uncoupled model wind speed (m/s) at 0:00 July 31. Black dots represent the center of the storm. QSCAT-NCEP winds are high-quality re-analysis winds obtained by a weighted blend of QSCAT and NCEP wind re-analysis fields (Morey et al. 2006). QSCAT is the satellite Quick Scatterometer data. NCEP is the National Centers for Environmental Prediction. The results show that the coupled model simulation with extensive open water is a better simulation of the best re-analysis result, the blended QSCAT-NCEP winds. Black line in **a** is used in vertical section in Figure 5

winds of ~16 m/s. These results suggest that the effect of surface fluxes from increased open water area is a stronger, larger storm, in agreement with re-analysis wind data, and in accord with Simmonds et al. (2008). By comparison, the uncoupled simulation, assuming climatology for ice cover, results in a smaller, less intense storm (by about 4 m/s), compared to the coupled simulation. The reduced sea ice in the coupled simulation causes an increase in solar radiation received by water, with lower albedo, and with warming mainly limited to the atmospheric boundary layer (Fig. 4). This reduces stability within the boundary layer, increasing momentum exchanges between the boundary layer and higher troposphere levels and increasing surface winds. However, as this process does not significantly change the atmospheric mass balance, changes in the central SLP remain small, compared to changes in surface winds (Fig. 3).

Surface air temperature is an important factor in estimating long-wave radiation and surface sensible heat flux. Because of high albedo, sea ice receives much less short-wave radiation than sea water. Thus, the surface air temperature is much warmer, in coupled model

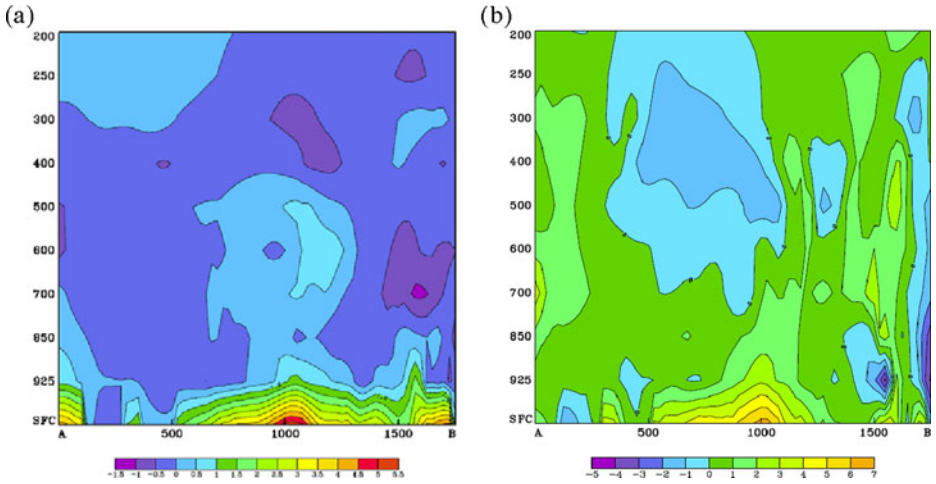

Fig. 4 Vertical profiles along the black line in Figure 4 for the differences between coupled model result *minus uncoupled model* result for (**a**) temperature, (**b**) wind speed at 0:00 July 31. Units are °C, and m/s for (**a**), and (**b**). Results show that the impacts of feedbacks in the coupled model simulation are mostly in the atmospheric boundary layer

simulations where a storm passes through over open water, than when the storm passes over ice. For this particular storm, the maximum difference in surface warming is up to 8°C due to the net impacts of increased solar radiation and surface mixing. In the atmosphere, the warming is largely confined to the boundary layer (<925 hPa), with difference in warming reaching ~5°C between the two simulations (Fig. 4a). For the 2008 storm, warming did reach upper levels, for example as much ~1°C near 600 hPa, suggesting increased boundary turbulence and reduction of stability.

Compared to more ice-covered conditions, increased winds associated with surface fluxes from the open water, are mainly limited to the boundary layer, with associated reductions in winds at upper levels, at about 250~500 hPa (Fig. 4b). Thus, reduced ice, and increased surface winds result in enhanced boundary layer instability and momentum exchange between the boundary layer and the mid- and upper troposphere levels. As with the 1999 storm, the 2008 storm resulted in a reduced sea surface temperature in the open waters of the Beaufort Sea, by up to 2°C, and essentially no temperature change in ice covered areas. Analysis of winds, temperature and currents show that the storm resulted in enhanced vertical upper-ocean mixing, bringing cold water to the surface and deepening the mixed layer.

2.3 Summary

Modeling studies were the focus of ImSAS, verified by in situ and remotely sensed data collected during collaborating projects. Results demonstrate that factors such as open water, ice, and ocean surface fluxes can modulate, and be modulated by, storms. Increased open water changes the air-sea fluxes and processes related to sea ice, relative to other processes, such as short and long wave radiation, seawater albedo, Arctic storm dynamics, moisture differences, cloudiness, ocean waves, and upper ocean dynamics including vertical mixing and upwelling. Large expanses of open water allow enhanced air-sea fluxes, of heat and momentum. The two storms presented in this paper are intended to describe the possible

impacts of future climate change with reduced sea ice, compared to past conditions; the 1999 storm with modest open water experiences less impacts from ocean surface fluxes than the 2008 storm with a large open water area. These results support the view that future climate change may result in larger more intense storms, as suggested by Simmonds et al. (2008).

3 Intercontinental Atmospheric Transport of Anthropogenic Pollutants to the Arctic (INCATPA)

3.1 Atmospheric transport and behaviour of toxic pollutants in the Arctic

POPs, e.g. polychlorinated biphenyls (PCBs), organochlorine pesticides (OCPs) and combustion by-products, and mercury (Hg) are toxic chemicals that persist in the environment and can be carried by air and water over long distances from emission sources (Hung et al. 2005; Macdonald et al. 2000). In the cold Arctic, these chemicals can be deposited onto surfaces and accumulate in wildlife, country foods and in people, and possibly have negative health impacts. The presence of these anthropogenic pollutants in the Arctic ecosystem has raised significant international concerns in recent years, especially in circumpolar countries. IPY- INCATPA was designed to assess the atmospheric input of these pollutants from external sources to the Arctic, focusing on intercontinental transport from the Pacific Rim, extending the existing international air monitoring network of the Arctic Monitoring and Assessment Programme (AMAP). One component of INCATPA was to couple measured atmospheric data from AMAP long-term monitoring stations with statistical analysis and model simulations, to elucidate how climate change would affect pollutant transport to, and behaviour within, the Arctic. Some of the major findings are summarized here.

The atmosphere is considered to be the primary and most rapid pathway of pollutant transport to the Arctic. Most legacy POPs have no sources in the Arctic. Therefore, their presence in the Arctic environment has been generally regarded as evidence of long-range transport (LRT). Atmospheric LRT events are able to move polluted air masses within a few days from source regions into the central Arctic region. For example, Eckhardt et al. (2007) reported PCBs released from biomass burning were observed in air at the Zeppelin Arctic station (Svalbard/Norway) after a travel time of a few days (from agricultural fires in Eastern Europe) to a few weeks (from boreal forest fires in North America). Measurements at the Polar Environment Atmospheric Research Laboratory (PEARL, see below) confirm transport from Southeast Russia to 80ºN in about 5 days (Saha et al. 2010). There is also evidence of LRT of Hg from industrial pollution from Asian sources to the north western United States (Weiss-Penzia et al. 2003).

POPs can partition to air, water, soil, snow/ice and other environmental media according to their physical-chemical properties. Cold temperatures can induce their deposition and accumulation in Arctic environmental media, thus resulting in the so-called cold-trapping effect (Rahn and Heidam 1981). Since their physical-chemical properties vary with temperature, climate change will affect their fate in the environment, influencing the observed concentrations and trends in the Arctic.

Discovery of atmospheric mercury depletion events (AMDEs) in the Arctic in spring (Schroeder et al. 1998) revolutionized the understanding of the atmospheric behaviour of Hg. During an AMDE, atmospheric conversion of gaseous elemental mercury (GEM) or Hg^0 creates increased amounts of reactive Hg^+ or Hg^{2+} and particulate -bound mercury deposited in the Arctic. Once deposited, mercury can be converted to highly toxic bioaccumulating methylmercury. Methylation can occur in aqueous environments such as oceans

(Sunderland et al. 2009), freshwater wetlands (Loseto et al. 2004; Goulet et al. 2007) and peatlands (Mitchell et al. 2008). It is speculated that factors affected by climate change, such as earlier ice breakup, increased snowmelt and warmer temperatures, may influence these conversion processes and, thus, the overall input of Hg to the Arctic environment and the bioaccumulation in wildlife and humans.

Here, long-term time series of POPs and mercury collected at AMAP stations were inspected using statistical methods to try to unveil evidence of climate change impacts in observed atmospheric levels and trends. Models were developed and parameterizations were improved to elucidate and forecast the climate change effects on these pollutants.

3.2 Evidence of climate change impacts on air concentrations of POPs and mercury

3.2.1 POPs

AMAP initiated atmospheric monitoring of POPs in the Arctic at 4 long-term air monitoring stations in the early 1990s (Hung et al. 2010). Measurements at Zeppelin, Svalbard (78°55′ N, 11°56′E) and Alert (82°30′N, 62°20′ W) are the longest datasets available to investigate climate change impact on POPs behaviour in the Arctic. Using a statistical Digital Filtration Technique to develop atmospheric time trends for POPs at AMAP stations, Hung et al. (2010) showed that from 1993 to 2005/2006 most POPs consistently exhibit declining trends in the air, and the decline has slowed at some stations in recent years. Since the 1970s, many countries have restricted the production, and usage of POPs (United States banned DDT in 1972), and these chemicals are now banned globally according to the Stockholm Convention on POPs of 2001. Thus, reduced air concentrations at specific Arctic locations could result from international controls, proximity to sources, environmental degradation and reactions, environmental transport pathways and residence times of a specific chemical in various media. Ma et al. (2011) suggest that apparently declining trends may have overwhelmed any effect that climate change may have on POPs in Arctic air. To reveal the underlying climate change impact, the decline due to factors other than climate change must first be removed.

It is expected that as the Arctic warms and sea ice retreats, previously deposited POPs may be re-mobilized from environmental repositories, e.g. snow/ice, soil and water, back into the atmosphere. Indeed, Wong et al. (2011) and Gioia et al. (2008) showed evidence of α-hexachlorocyclohexane (α-HCH, a pesticide) evading over open water in Hudson Bay and the Beaufort Sea, and increases in PCB air concentration at the ice edge in the Atlantic Arctic. For some POPs, e.g. hexachlorobenzene (HCB), and some PCBs, increasing atmospheric trends were observed at Zeppelin and Alert in early- to mid-2000s which may result from enhanced volatilization from the ocean due to ice retreat (Hung et al. 2010). Increasing trends were only observed for these chemicals but not others, implying higher tendencies to volatilize from water. In search of climate change impacts on POPs distributions in the Arctic, Ma et al. (2011) used a statistical de-trending method to remove the dominant declining trends from the time series of 10 selected POPs measured at Alert and Zeppelin, which did not show apparent increasing trends. After detrending, most POPs show increasing tendencies that correspond well to surface air temperature (SAT) and sea ice concentration. An example of the detrended and observed data for α-HCH at Zeppelin is shown in Fig. 5. After 2000, when sea ice retreat sped up, detrended POPs air concentration began to have positive correlations with SAT and negative correlations with sea ice concentration at significance levels of ≥90 % in the summertime (June-August), when ice-melt is maximal and atmospheric input from southerly sources is less important. Ma et al.'s findings imply that chemical repositories in water, snow/ice and soil may return these toxic chemicals to the

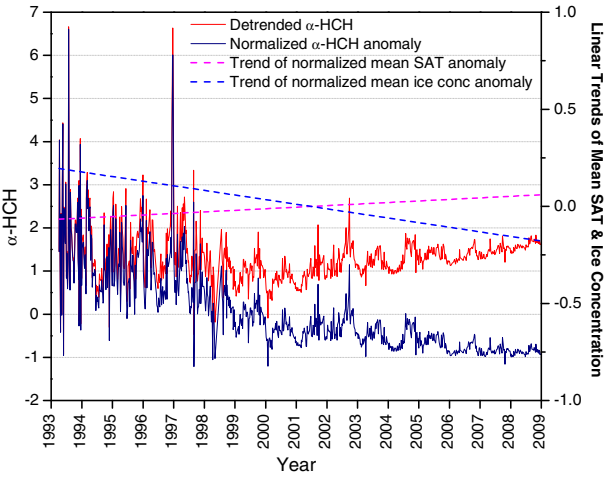

Fig. 5 Detrended (residual) and normalized (by standard deviation) time series of weekly sampled air concentration anomalies of α-HCH ($pg \cdot m^{-3}$) between 1993 and 2009 at Zeppelin. Also shown are linear trends of normalized mean air temperature anomaly (*pink dash line*) and normalized mean ice concentration (*blue dash line*) over the Arctic. (Adopted from Ma et al. (2011) Fig. 1a)

air under climate change, making them once again available for circulation. Arctic warming potentially may undermine global efforts to reduce environmental and human exposure to POPs.

3.2.2 Mercury

Long-term monitoring of atmospheric mercury at Alert is the longest continuous dataset collected in the Arctic. Cole and Steffen (2010) attempted to identify climate change effects by analyzing statistical changes in concentrations from 1995 to 2007 at this site. They showed that Arctic springtime AMDEs were occurring earlier in the spring in recent years (Figure S4). On average, AMDEs during 1996 to 2002 occurred 14 % of the time in March, 36 % in April, and 45 % in May, with a small number in February and June. During 2003–2009, 26 % of AMDEs occurred in March, 40 % in April, and 29 % in May. The total number of AMDEs did not change significantly. The cause of this AMDE shift to earlier spring occurrences is not clear; however, the chemistry that drives these events has been linked to fresh sea ice and low air temperatures. Therefore, climate change may be driving the shift—and changing patterns of mercury deposition to the Arctic ecosystem—through trends in air temperatures, changes in sea ice composition and extent, earlier snowmelt, changes in atmospheric transport patterns, or related processes.

In addition to trends in AMDE timing, the analysis of the long-term mercury data sets at Alert and Amderma (Russia), show that mercury concentrations at both locations correlate with the local temperature within each of the spring months (Fig. 6; Cole and Steffen 2010). While this is consistent with earlier reports that some of the steps involved in AMDE chemistry may be temperature-dependent, there are many factors that affect atmospheric mercury concentrations. Therefore it is too soon to predict the net effect of climate change on future mercury deposition to the Arctic. However, these results show that continued study of AMDE chemistry and continued monitoring of Arctic mercury is necessary in a changing climate.

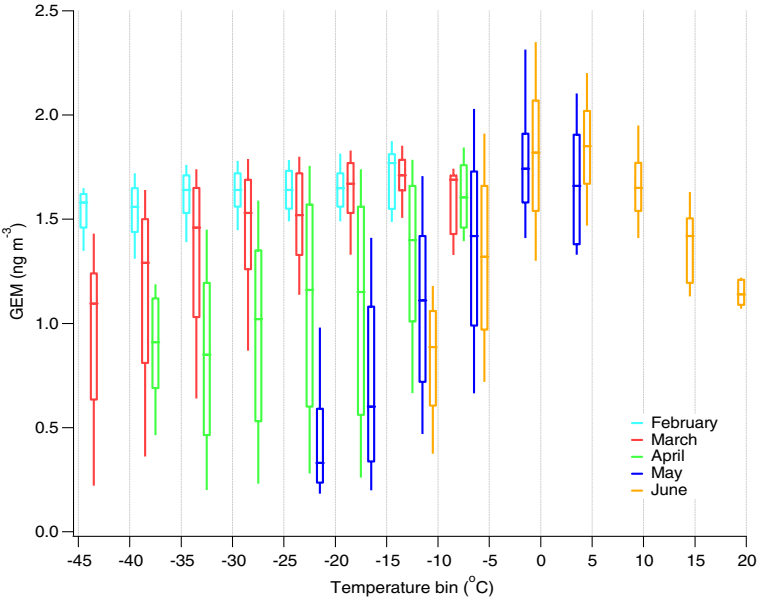

Fig. 6 Box and whisker plot of spring gaseous elemental mercury (GEM, or Hg0) concentrations at Alert based on month and air temperature. Temperature is binned in 5 ° increments. Boxes represent 25th and 75th percentiles; whiskers represent 10th and 90th percentiles. Data are hourly mean concentrations from 1995 to 2009

3.3 Modelling climate change impact on toxic pollutants and implications

3.3.1 POPs

From long-term measurements at Alert and Zeppelin, Ma et al. (2011) showed that POPs may be volatilizing from Arctic environmental reservoirs as a result of climate change. To further elucidate this enhancement in secondary sources and to understand the difference in extent of volatilization, a perturbation model for POPs concentrations in closed air-water/air-soil systems was developed to quantify the effects of climate change perturbation (Ma and Cao 2010). This model was then extended to illustrate exchange in a closed air-snow/ice system (see Ma et al. 2011 for details).

The model was designated to simulate the response of POPs to climate change by assuming that chemical concentration in an environmental compartment is equal to the sum of mean concentration and perturbed concentrations induced by climate change. The mean concentration in the model is allowed to change, subject to degradation under a mean temperature, and the perturbed concentration is simulated through environmental removal and air-surface exchange dynamics, subject to temperature and precipitation anomalies incurred by climate change. The perturbed air concentrations have been evaluated extensively by comparison with detrended POP air concentrations measured over the Great Lakes and the Arctic (Ma and Cao 2010; Ma et al. 2011). Results show that perturbed atmospheric α-HCH concentration increases and remains high till 2037, then decreases due to degradation (Fig. 7). Modeled results of perturbed α-HCH air concentrations correlate well with the detrended time series between 1999 and 2009 at Zeppelin (r=0.66; p=0.028), indicating reasonable projected perturbations of POPs under the 21st century IPCC A1B climate

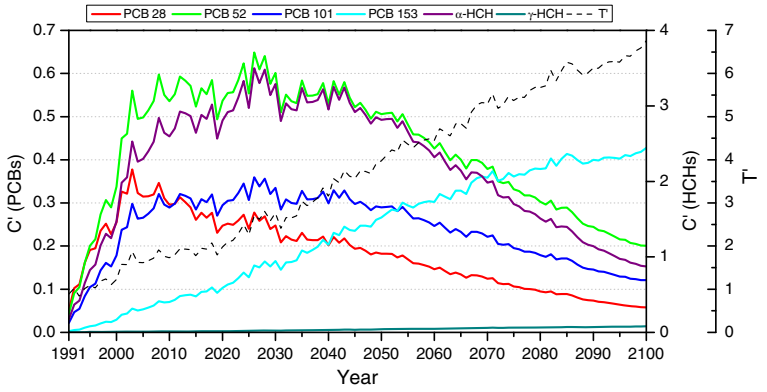

Fig. 7 Modeled perturbed annual air concentrations of HCHs and PCBs in the closed air-water system (1991–2100) under the IPCC multi-models ensemble average of annual SAT anomalies (°C) over the Arctic, for SRES A1B climate change scenario. Annual SAT anomalies are shown in black dashed line and scaled on the second right y-axis, HCHs (scaled on the first right y-axis) and PCBs (scaled on the left y-axis) are shown in colored solid lines. (Adopted from Ma et al. (2011) Fig. 2)

change scenarios. PCB 153 and γ-HCH showed apparently different trends than the other PCBs and α-HCH. PCB 153 is more hydrophobic and γ-HCH is more water soluble than most of the other compounds. These properties allow them to stay in environmental reservoirs (e.g. sediment/soil and water) for longer periods of time.

3.3.2 Mercury

Once emitted, mercury can be transported via the atmosphere, undergo atmospheric transformation and deposit on the Earth's surface. Mercury deposited onto the cryosphere (snow/ice) may revolatilize back to the air, remain in long-term cryospheric records (firn/glaciers) or be entrained into meltwater. Mercury in meltwater may enter Arctic lakes and oceans where it can be converted to methylmercury and bioaccumulate through the food chain. There are great uncertainties in what fraction of mercury deposited onto the cryosphere is emitted back to the atmosphere and what fraction goes to meltwater. In order to reliably predict the effect of climate change on mercury input and circulation in the Arctic, physical and chemical processes involved in the deposition, chemical transformation within the cryosphere and emission must be depicted accurately in environmental models. To date, the only model to represent dynamically the physical and chemical processes that determine the fate of mercury deposited onto snowpacks was described by Durnford et al. (2012b). The model was able to reproduce observed concentrations of mercury in snowpacks and snowpack meltwater runoff. The inclusion of the dynamic snowpack mercury model improved the simulation of the Global/**R**egional **A**tmospheric **H**eavy **M**etals (GRAHM) Model for the wintertime atmospheric mercury concentrations, including high-latitude AMDEs. Durnford and Dastoor (2011) reviewed published observations of cryospheric mercury concentrations and found that GEM deposited onto the cryosphere is likely revolatilized immediately; deposited particulate mercury is likely retained by the snowpack. Deposited reactive gaseous mercury (Hg^{+} or Hg^{2+}) may be reduced to GEM which is partially emitted and partially reoxidized and retained by the snowpack. Durnford et al. (2012a) statistically analyzed the relationship between observed mercury concentrations and simulated environmental parameters and found that the presence of cryospheric halogens impacts the behaviour of

cryospheric mercury significantly. Cryospheric mercury observations were found to be most strongly controlled by the dry and wet depositions of oxidized mercury, with burial by fresh snowfalls and wind driven ventilation of snowpacks being important processes.

The complexity of these processes makes it difficult to speculate on the net effect of climate change on the deposition and accumulation of mercury in Arctic ecosystems. For example, it is uncertain whether AMDEs would occur more or less frequently (Durnford and Dastoor 2011). In a warming Arctic, the optimal season for AMDEs to occur will become shorter, when sea ice refreezes in the presence of sunlight, resulting in fewer AMDEs. Yet, during this shorter AMDE season, thinner and more dynamic sea ice, forming leads and refreezing more frequently, may result in more frequent AMDEs. Development of physical and chemical processes of mercury in the cryosphere and at the atmosphere-cryosphere interface in mercury fate models needs to continue in order to better understand/quantify how climate change may affect mercury input to the Arctic.

4 Ocean Atmosphere Sea Ice and Snow interactions in polar regions (OASIS)

The IPY project OASIS focused on the atmosphere-ice-ocean interface; it was conceived to address deficiencies in the understanding of the chemistry that occurs over the Arctic Ocean surface, and the lack of measurements. The changing nature and extent of sea ice (Maslanik et al. 2007; Nghiem et al. 2007), dramatic shift from multi-year to more saline seasonal ice, and increased density of open leads, increasing the heat flux from ocean to atmosphere, could have a profound impact on the physical and chemical processes that occur in the ice, and on its surface and overlaying atmosphere.

Two surprising discoveries were made in the late 20th century at the world's most northerly atmospheric observatory at Alert, Nunavut. Firstly, it was observed at Alert (Bottenheim et al. 1986) and Barrow, Alaska (Oltmans and Komhyr 1986) that ozone (O_3), a toxic greenhouse gas, occasionally completely disappeared from the lower atmosphere during in the spring. These so-called ozone depletion events (ODEs) have been shown to be related to bromine chemistry (Barrie et al. 1988). The second surprise, in the mid-1990s, was the concurrent decrease of GEM during ODEs (Schroeder et al. 1998). Ongoing research at Alert and other Arctic observatories has made it clear that bromine involved in these disappearing acts came from sea salt in a process that most likely started over the ocean (Simpson et al. 2007a). However many of the details of the chemical processes at play were not well understood, and this was not helped by the scarcity of actual in-situ measurements over the Arctic Ocean. Furthermore, there was virtually no information on the behavior and abundance of carbon dioxide (CO_2) over the frozen ocean. While satellite remote sensing has provided extensive spatial coverage of the concentrations of some pollutants over the Arctic Ocean, the detection of CO_2, O_3 and GEM at a spatial and temporal resolution required to investigate their chemical processes is beyond the capabilities of satellites, and thus, in-situ measurements are indispensable.

One focus of OASIS was to develop methods to measure O_3, GEM, bromine oxide (BrO, a convenient, measurable tracer for bromine chemistry) and a set of meteorological parameters including flux and radiation, over the ocean, and deploying the equipment from ships, ice-breakers, fixed wing aircraft and helicopters. Thus, the Out On The Ice (OOTI) concept was developed, consisting of a specially designed miniature atmospheric chemistry and physics laboratory, mounted on a sled for rapid snowmobile deployment, for measurements on the ice. Also, an ice-tethered buoy, the "O-buoy", was designed in cooperation with Knepp et al. (2010) to make long term autonomous measurements (>1 year). The O-buoys contain an accurate CO_2

detector, and O3 and BrO instrumentation. With OOTI, O-buoys, and more standard equipment, a large dataset was obtained that will improve the understanding of physical and chemical processes in the air over the Arctic Ocean, help constrain models used for predicting change and permit development of scenarios for the future in the face of a changing climate. The first results from the OASIS activities during IPY are summarized below.

4.1 Ozone

IPY brought unprecedented opportunities to expand the previously limited record of O_3 depletions over the Arctic Ocean (Hopper et al. 1992, 1998; Ridley et al. 2007; Morin et al. 2005; Jacobi et al. 2006). Platforms for measurements included a sail boat frozen into the ice to make 16 month-long O_3 observations (Bottenheim et al. 2009), O-buoys (Bottenheim et al. 2010), the Canadian Coast Guard Ship Amundsen, collaborating with the IPY Circumpolar Flaw Lead study (Barber et al. 2010), a sea ice camp near Kuujjuarapik/Whapmagoostui, Quebec as part of the Impact of Combined Iodine and Bromine Release on the Arctic Atmosphere (COBRA) campaign (NERC 2009) a sea ice camp near Barrow, Alaska, as part of OASIS-09, and the Polar-5 aircraft as part of the Polar Airborne Measurements and Arctic Regional Climate Model Intercomparison Project (PAM-ARCMIP), collaborating with the Alfred Wegener Institute, Germany, (Herber et al. 2012).

Among the most profound results was confirmation that the normal state of (ground level) O_3 over the springtime Arctic Ocean is a depleted state (Bottenheim et al. 2009). However, the synoptic meteorological conditions required for ODEs were still not resolved. Jacobi et al. (2010) investigated the correlation between these widespread depletions and mesoscale synoptic conditions and found that they are frequently associated with high pressure systems. While the correlation of O_3 with pressure in their study was stronger than that with temperature, the Amundsen data show a strong temperature correlation (Seabrook et al. 2011).

One controversy pertains to the question where the depletion chemistry starts, and whether decreases in the O_3 (and GEM) concentration observed at a fixed location is due to local depletion chemistry, or reflects a change in air mass with different levels of O_3 (and GEM). In-situ flux experiments with the OOTI sled near and right over frost flowers did not show any noticeable decrease in the O_3 concentration close to the surface (~10 cm) in comparison to that at 2 m above the surface. This suggests no tendency to depletion near frost flowers, in agreement with Piot and von Glasow (2008). Eddy covariance experiments with a fast ozone detector on the ice near the Amundsen ice breaker, and at an ice camp near Barrow showed a similar negligible O_3 "deposition" rate. Some anecdotal evidence obtained during the Polar-5 flights in 2009 suggested that suspended ice particles ("diamond dust", possibly generated from frost flowers by wind erosion) were negatively correlated with O_3, implying that some of the chemistry may occur in the troposphere rather than at the surface. What is certain is that either the destruction itself happens on the surface, or that the precursors of the destruction mechanism originate from there (Seabrook et al. 2011).

4.2 Mercury

GEM is known to deplete in the atmosphere but, unlike O_3, is not destroyed but converted into another chemical state of mercury (Hg). As a result of similar halogen chemistry that destroys ozone, GEM is oxidized to an inorganic reactive gaseous mercury (RGM) species (Steffen et al. 2008). RGM is very 'sticky' and therefore can readily deposit on snow and ice surfaces through dry deposition. It can also easily associate to particles in the air and deposit on a surface as "particulate Hg" (PHg). However, it was found that after deposition, RGM and PHg can be

reduced back to GEM and re-emitted from a snow surface back into the atmosphere to be transported or oxidized again (Lalonde et al. 2003; Poulain et al. 2004). This cycle of reduction and re-emission has been found to occur at the near snow/ice surface (Steffen et al. 2002). OASIS set out to determine whether this Hg cycle, observed at inland snow packs (from where all previous studies have been reported), differs on the sea ice and close to ice leads.

Results show that there is significantly more PHg over sea ice than is generally observed inland, implying a greater impact on exposure of the Arctic Ocean to Hg deposition. If most deposited Hg is re-emitted to the atmosphere, as suggested by Kirk et al. (2006), then Hg deposition would not constitute a great contribution to the Arctic ecosystem as previously suggested (Lu et al. 2001). However, real time measurements from OASIS found that the re-emission of GEM is substantially suppressed over sea ice when simultaneously compared to emissions over the inland snow pack. Thus, much more deposited Hg appears to be retained over sea ice than over land-based snow pack. Consequently, models estimating the contribution of Hg from the atmosphere to the Arctic Ocean and the Arctic as a whole may need to be reassessed.

4.3 Bromine monoxide (BrO)

BrO is exclusively produced from the reaction between O_3 and bromine atoms (Br). As this reaction is assumed to be the main driver for O_3 depletion, BrO is a prime marker for the occurrence of this depletion. Regions of enhanced total column of BrO captured by satellites and aircraft over Polar Regions (Wagner and Platt 1998; Richter et al. 1998, 2002; McElroy et al. 1999) have been associated with bromine emission from sea-salt aerosols, frost flowers, ice leads and salt covered snow (Kaleschke et al. 2004; Simpson et al. 2007b). So-called BrO clouds have been observed for many days over large areas, suggesting an efficient air mass transport mechanism (Begoin et al. 2010). However, it is not clear if large-scale elevated BrO clouds are due to continuous generation from the surface as the air traverses the source region, or if high BrO is sustained in the air during transportation away from a surface source. In fact it has recently been argued that much of the BrO seen by satellites is not related to lower tropospheric BrO (Salawitch et al. 2010). Thus, it is important to determine the presence of in-situ lower troposphere BrO.

With the OOTI sled, ground-based measurements were made at two High Artic locations (Amundsen Gulf and Barrow) and one sub- Arctic location (Kuujjuarapik/Whapmagoostui, Quebec). Previous ground based observations at Alert showed a strong negative correlation between measured O_3 and BrO (Hönninger and Platt 2002). In these IPY campaigns, the OOTI studies also showed that in many cases O_3 levels were negatively correlated with BrO. However, elevated BrO levels were observed during periods when no ODE was present or O_3 concentrations increased to background level. Furthermore, O_3 wasn't always entirely destroyed in the presence of very high BrO levels; in fact ODEs were recorded with BrO below the detection limit of the instrument (Pöhler et al. 2010). It was also observed that O_3 often decreased quickly while BrO increased when a low pressure system center moved over the measurement site. Ongoing analysis focuses on the extent that these variations agree with satellite data (Netcheva, in preparation 2012).

4.4 Surface-Atmosphere exchange

Surface-atmosphere interactions over the Arctic Ocean are modulated by unusual dynamic conditions. The absence of direct insolation during the polar night, coupled with radiative cooling of the surface, results in stable stratification of the boundary layer and therefore

suppression of turbulence and vertical mixing. This condition persists well after polar sunrise because of the low sun angles at these latitudes and has profound implications for transports of atmospheric constituents towards or away from the surface.

Under stable conditions, surface fluxes are difficult to determine because commonly used empirical relationships between vertical gradients and the turbulent fluxes of wind (momentum), temperature and atmospheric constituents are not well defined. Prior to IPY, only a handful of studies addressed these difficulties which calls into question how representative each study was of general conditions in polar regions (cf. Yagüe et al. 2001; Grachev et al. 2005, 2007; Sodemann and Foken 2005; Lüers and Bareiss 2010).

Results from IPY indicate that as long as gradient and turbulent flux measurements are within a few meters of the surface, prevailing winds produce enough momentum to provide mixing at least 60 % of the time (Staebler, to be submitted 2012). At 0.6 m height, very stable conditions are observed only 10 % of the time. At higher altitudes, flux divergence results in more severe underestimations of surface fluxes. From the surface layer (~10 m) to the top of the boundary layer (~200 m), dynamically stable stratification with Richardson numbers well above 1 usually persist. IPY ozone profiles helped clarify the part of the atmosphere in direct contact with the surface on time scales of hours or less. Typical ozone-depleted layer depths at Barrow in 2009 were 100~800 m with an average very close to the average inversion height, 380 m.

4.5 IPY legacy: OOTI, O-Buoy, PAM-ARCMIP

To obtain insight to the atmospheric composition of the surface boundary layer over the Arctic Ocean, it was necessary to develop methodologies to make fully autonomous observations. This required that the equipment operate on batteries, be very economic in power consumption, and be controlled by remote access. The development of the OOTI technology was highly successful in this regard. These concepts proved very helpful in overcoming initial reservations towards the development of the O-buoys that would have to operate over much longer periods of time (fully autonomous for periods of up to 2 years). The major new aspect of O-buoys is the capability to make chemical composition measurements of the atmosphere, which posed a very complicated engineering undertaking, substantially different from existing ice-tethered buoys in the Arctic.

The OOTI system has successfully operated during OASIS-CANADA campaigns and has been invited to participate in future Arctic campaigns. The first O-buoys were deployed and operated successfully for up to 10 months in the Beaufort Sea as a “proof of concept”. A much expanded deployment program was recently funded by US partners with construction and deployment of 15 additional O-buoys over the next few years. Another IPY legacy is a collaborative international pan-Arctic flights program in the spring with the Polar-5 aircraft (Herber et al. 2012). The 1st prototype campaign incorporating flights from Longyearbyen (Svalbard) via Alert to Barrow took place in spring 2009 with OASIS-CANADA participation; a 2nd campaign was conducted in spring 2011. The success of those flights resulted in the extension of several years of similar projects, hopefully eventually encompassing a complete circum-polar flight plan.

5 Our PEARL near the pole

The Polar Environment Atmospheric Research Laboratory (PEARL) is located at Eureka (Figure S5) in Nunavut (80°N, 86°W). In 2005, the Canadian Network for the Detection of

Atmospheric Change (CANDAC), a collaboration between universities and government departments, began operations, which were intensified during IPY.

PEARL is a "whole atmosphere" laboratory containing instrumentation to study the atmosphere from the ground to about 100 km. It comprises three sites: (1) the Ridge Laboratory 600 m above sea level is used mainly for upward-looking remote sounding experiments, (2) the zero altitude PEARL auxiliary laboratory (ØPAL) at approximately sea level is mainly used for boundary layer and near-surface measurements, and (3) the Surface Atmospheric Flux and Irradiance Remote Extension (SAFIRE) site used for experiments that need to be far from any outside human interference.

The PEARL equipment roster includes lidars, radars, spectrometers, and optical instruments suitable for active and passive probing of the atmosphere, its physical and radiative states, and its composition. Several of the PEARL instruments have been certified as part of international networks of instruments. In addition to the instruments located at PEARL, researchers have been able to take advantage of PEARL's location as a favoured site for satellite over-flights to expand the available data for this location (Figure S6). One IPY research project measured clouds, rain and snow in the Arctic via satellites, where precipitation is much different from lower latitudes. High-quality data collection can occur if a synoptic storm passes over the laboratory. Ground-based data guided the development of specific Arctic algorithms, e.g. verifying the importance of the attenuation correction of the CloudSat W-band radar data. It was also possible to improve the inputs into atmospheric models by better understanding the atmosphere's composition above Eureka by measuring the absorption of solar radiation by the atmosphere. Ozone and related gases have been regularly measured by this method throughout IPY.

Being able to acquire a lengthy period of data during IPY allows comparison with measurements taken in different parts of the Arctic. This was the first time that upper atmosphere mean winds, and diurnal and semi-diurnal atmospheric tides were studied at true Polar Arctic locations using contemporaneous longitudinally spaced systems. It was found that the winds and tides are asymmetric, or vary with longitude, indicating the presence in the monthly means of relatively large stationary planetary waves at middle atmospheric heights (20–80 km). Their nonlinear interactions with the tides created large non-migrating tides. Studies of the variability and possible couplings of the semi-diurnal tides in the Northern and Southern Hemispheres provided some unexpected results. For example, Northern Hemispheric winter stationary planetary waves provide non-migrating tides for Antarctica, but the reverse is not true (Xu et al. 2009a, b; Manson et al. 2009).

A working relationship and collaborative projects were developed with members of Eureka's sister observatory in the European Arctic, whereby researchers from the Alfred Wegener Institute (AWI) carry out regular lidar, sunphotometry and starphotometry measurements at Ny Alesund, Spitsbergen (78°55′24″N, 11°55′15″E) and similar measurements were made at Eureka. A preliminary initiative to characterize polar winter and polar spring aerosols at both sites using lidar and starphotometry, supported by a circumpolar, AWI-led airborne lidar program and pan-Arctic, 2D CALIOP profiles, was begun in 2009 with the implementation of a starphotometer at Eureka alongside the Arctic High Spectral Resolution Lidar (AHSRL). The collaborative program has led to significant findings related to the pan-Arctic characterization of the abundance and size of (a) spring-time Arctic Haze aerosols using airborne sunphotometry data from multi-altitude circumpolar flights (Saha et al. 2011) and (b) stratospheric sulphate aerosols from the Russian Sarychev volcano that erupted in June of 2009 (O'Neill et al. 2011).

PEARL research also improved our ability to track the spread of smoke and pollution from the lower part of the atmosphere to the upper part, where they can affect weather and

climate. This is important because presently there is only a generic, phenomenological understanding of the sources and nature of the complex upper-tropospheric turbidity patterns that develop when aerosols are transported into the Arctic. Detection of plumes over PEARL from fires at more southern latitudes show significant atmospheric transport towards the poles. A spectacular illustration of such polar meridional transport and the attendant altitude-dependent complexity of tropospheric turbidity patterns can be seen in Fig. 8. A mosaic of MODIS images was employed to capture a pan-Arctic smoke plume that had been transported from southeast Russia to Eureka in about 5 days (Saha et al. 2010). An AEROCAN/AERONET sunphotometer and the Arctic High Spectral Resolution Lidar (AHSRL) simultaneously captured this plume as it passed over Eureka at altitudes between about 5 and 9 km. Optical signatures in this data, notably the dominance of sub-micron particles (red trace in the upper left-hand plot) and low AHSRL depolarization ratio (bottom left-hand figure) confirm other supporting data in establishing that this plume consisted of Russian smoke particles. Our ability to trace and deconvolve the aerosol properties of such plumes is an essential element in understanding the dynamics of Arctic aerosol intrusions and the climatic influences of the fundamental radiative forcing constituents. Stratospheric aerosol analysis software was developed and applied to several years of Polar sunrise (February-March) lidar measurements taken at Eureka. From statistics of the layering, it was found that aerosol layers in the lower stratosphere are typically ice while in the middle stratosphere they are particles of volcanic, or possibly forest fire origin.

One of the advantages of the intense operation of PEARL was the collection of data during the polar night. There is much less data available during night conditions than day, as

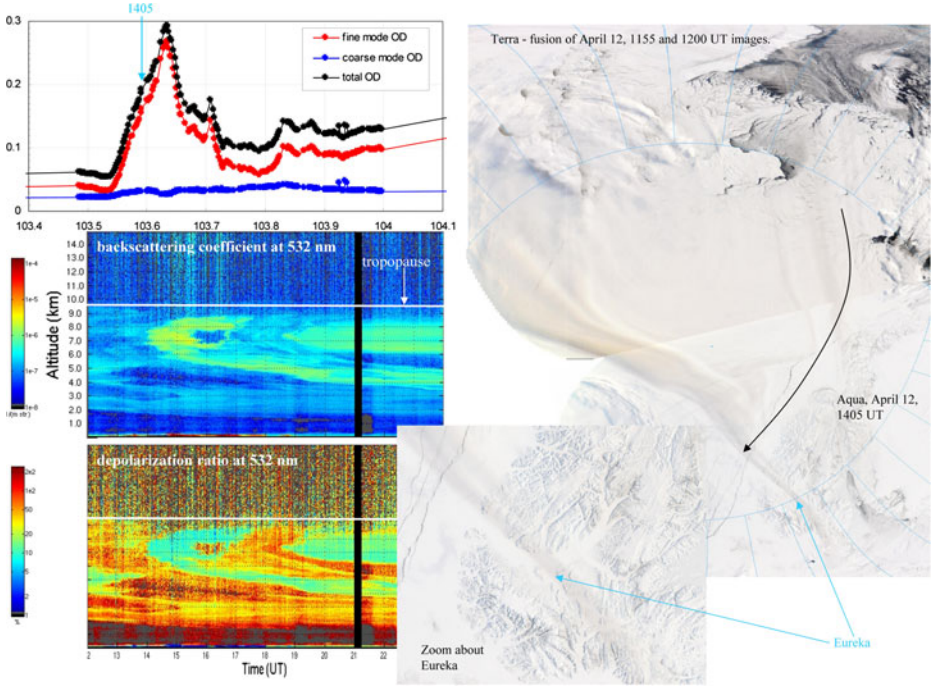

Fig. 8 AEROCAN/AERONET sunphotometer data (*top, left*) and the Arctic High Spectral Resolution Lidar (AHSRL) backscatter (*middle, left*) and depolarization ratio (*bottom, left*) plots on April 12, 2008. On the right side is a fusion of MODIS images from Terra and Aqua with an inset (*bottom, right*) zoom over Eureka

it is much more difficult to acquire. Analysis shows differences in temporal trends between summer and winter, which are not uniform throughout the year (Lesins et al. 2010), and evidence of strong water vapour intrusions into the Arctic in winter (Doyle et al. 2011). Bourdages et al. (2009) used lidar and radar to measure cloud properties. Different cloud types were identified and regimes included boundary layer ice crystals and ice clouds. Mixed-phase clouds and supercooled layers were also observed in March when temperatures were still extremely low (surface temperature of ~ −44°C).

The development of PEARL allowed a much wider range of atmospheric research at these extremely high latitudes than would have been possible otherwise. In addition, the year-round nature of the measurements corrects an inherent bias towards the summer months in most Polar data. PEARL also directly addresses the IPY objective of leaving a legacy of observing sites, and facilities to support ongoing polar research and monitoring.

6 Concluding remarks

Considerable new research is emerging on the role of climate, and its variations, on all components of the Arctic environmental system. For example, ImSAS demonstrated the importance of links between climate change, sea ice, cyclone properties, and the impacts of surface fluxes of momentum and enthalpy on cyclones that need better understanding. Further studies of wind and storm regimes will assist in gaining realistic assessments of possible changes in coastal impacts along the Beaufort and related Archipelago coasts. Studies of synoptic circulations, surface fluxes and the upper ocean are keys to better simulations and forecasts, on synoptic to decadal time-scales.

Results from INCATPA, studying intercontinental atmospheric transport of anthropogenic pollutants to the Arctic, were remarkable in finding that Arctic warming might remobilize POPs and augment mercury deposition/retention in the environment, undermining global efforts to reduce environmental and human exposure to these toxic chemicals. This was achieved through long-term atmospheric monitoring datasets, and climate change studies. Climate change may alter the risks of these toxic chemicals to different environmental media, humans and wildlife. Continued study of the relevant physical and chemical processes is essential to understand the role of climate change, and the impact of contaminant fate and risks, beyond time scales of present data.

OASIS established key baselines and methodologies to provide insights into the composition, properties and basic dynamics of the atmospheric surface boundary layer over the Arctic Ocean. Development of needed methodologies and technology is ongoing and will continue with new campaigns, for example, further development of the OOTI technology and the O-buoys, to operate autonomously for long time periods. Airborne pan-Arctic experiments will expand the observations, and lead to better modeling and forecast capability.

PEARL at Eureka has provided year-round monitoring of the entire atmospheric column from ocean surface to stratosphere, its physical and radiative states, composition, and tele-connections to lower latitudes, providing important in situ and atmospheric column data for comparisons with satellite data. Data sets include clouds, rain and snow, ozone and other gases, solar radiation, in the Arctic where these variables and parameters are much different from mid-latitudes, or tropics. These measurements provide extensive, multi-element datasets throughout the year for further atmospheric studies.

Acknowledgements These IPY projects were funded by the Government of Canada IPY Program. INCATPA thanks the Canadian Forces Station Alert for supporting data collection, acknowledges financial support for air measurements at Zeppelin from the Norwegian Pollution Control Authorities and at Alert from the Northern Contaminants Program (Indian and Northern Affairs Canada). ImSAS thanks the Panel on Energy Research and Development for funding of in situ field experiments by S. Solomon, off the Mackenzie Delta.

References

Arctic Climate Impact Assessment (ACIA) (2004) Impacts of a warming arctic: arctic climate impact assessment. Cambridge University Press

Barber DG, Asplin M, Gratton Y, Lukovich J, Galley R et al (2010) The International Polar Year (IPY) Circumpolar Flaw Lead (CFL) system study: introduction and physical system. Atmosphere-Ocean 48:225–243. doi:10.3137/OC317.2010

Barrie LA, Bottenheim JW, Schnell RC, Crutzen PJ, Rasmussen RA (1988) Ozone destruction and photochemical reactions at polar sunrise in the lower Arctic atmosphere. Nature 334:138–141

Begoin M, Richter A, Weber M, Kaleschke L, Tian-Kunze X et al (2010) Satellite observations of long range transport of a large BrO plume in the Arctic. Atmos Chem Phys 10:6515–6526. doi:10.5194/acp-10-6515-2010

Bourdages L, Duck TJ, Lesins G, Drummond JR, Eloranta EW (2009) Physical properties of High Arctic tropospheric particles during winter. Atmos Chem Phys 9(18):6881–6897

Bottenheim JW, Gallant AG, Brice KA (1986) Measurements of NOy species and O3 at 82° N latitude. Geophys Res Lett 13:113–116. doi:10.1029/GL013i002p00113

Bottenheim JW, Netcheva S, Morin S, Nghiem SV (2009) Ozone in the boundary layer air over the Arctic Ocean: Measurements during the TARA expedition. Atmos Chem Phys 9:4545–4557

Bottenheim JW, Matrai PA, Netcheva S, Perovich DK, Shepson PB et al (2010) Long term measurements of ozone, bromine monoxide and carbon dioxide over the frozen Arctic Ocean surface: first data from o-buoy deployments. Poster presented at the Annual Meeting of the American Geophysical Union, San Francisco

Brunner RD, Lynch AH, Pardikes JC, Cassano EN, Lestak LR et al (2004) An Arctic disaster and policy implications. Arctic 57:336–346

Caya D, Laprise R (1999) A semi-implicit semi-Lagrangian regional climate model: the Canadian RCM. Mon Weather Rev 127:341–362

Cole AS, Steffen A (2010) Trends in long-term gaseous mercury observations in the Arctic and effects of temperature and other atmospheric conditions. Atmos Chem Phys 10:4661–4672

Doyle JG, Lesins G, Thackray CP, Perro C, Nott GJ, Duck TJ, Damoah R, Drummond JR (2011) Water vapor intrusions into the High Arctic during winter. Geophys Res Lett 38:L12806. doi:10.1029/2011GL047493

Durnford DA, Dastoor AP (2011) The behavior of mercury in the cryosphere: a review of what we know from observations. J Geophys Res 116:D06305. doi:10.1029/2010JD014809

Durnford DA, Dastoor AP, Ryzhkov A, Poissant L, Pilote M, Figueras-Nieto D (2012a) How relevant is the deposition of mercury onto snowpacks?—Part 2: a modelling study. Atmos Chem Phys 12:2647–2706. doi:10.5194/acpd-12-2647-2012

Durnford DA, Dastoor AP, Steen AO, Berg T, Ryzhkov A, Figueras-Nieto D, Hole LR, Pfaffhuber KA, Hung H (2012b) How relevant is the deposition of mercury onto snowpacks? Part 1: a statistical study on the impact of environmental factors. Atmos Chem Phys Discuss 12:387–439. doi:10.5194/acpd-12-387-2012

Eckhardt S, Breivik K, Manø S, Stohl A (2007) Record high peaks in PCB concentrations in the Arctic atmosphere due to long-range transport of biomass burning emissions. Atmos Chem Phys 7:4527–4536

Gioia R, Lohmann R, Dachs J, Temme C, Lakaschus S et al (2008) Polychlorinated biphenyls in air and water of the North Atlantic and Arctic Ocean. J Geophy Res-Atmos 113:D19302. doi:10.1029/2007JD009750

Goulet RR, Holmes J, Page B, Poissant L, Siciliano SD et al (2007) Mercury transformations and fluxes in sediments of a riverine wetland. Geochim Cosmochim Acta 71:3393–3406. doi:10.1016/j.gca.2007.04.032

Grachev AA, Fairall CW, Persson POG, Andreas EL, Guest PS (2005) Stable boundary-layer scaling regimes: the SHEBA data. Boundary Layer Meteorol 16:201–235

Grachev AA, Andreas EL, Fairall CW, Guest PS, Persson POG (2007) SHEBA flux-profile relationships in the stable atmospheric boundary layer. Boundary Layer Meteorol 124:315–333

Herber A, Haas C, Stone R, Bottenheim J, Liu P, Li S-M, Staebler R, Strapp W, Dethloff K (2012) Regular airborne surveys of sea ice and atmospheric properties in the Arctic, EOS, in press

Hibler WD (1980) Modeling a variable thickness sea ice cover. Mon Weather Rev 108:1943–1973

Hönninger G, Platt U (2002) Observations of BrO and its vertical distribution during surface ozone depletion at Alert. Atmos Environ 36:2481–2489

Hopper J, Peters B, Yokouchi Y, Niki H, Jobson B et al (1992) Chemical and meteorological observations at ice camp SWAN during Polar Sunrise Experiment 1992. J Geophys Res 99:D12. doi:10.1029/94JD02303

Hopper J, Barrie L, Silis A, Hart W, Gallant A et al (1998) Ozone and meteorology during the 1994 Polar Sunrise Experiment. J Geophys Res 103:D1. doi:10.1029/97JD02888

Hung H, Blanchard P, Halsall CJ, Bidleman TF, Stern GA et al (2005) Temporal and spatial variabilities of atmospheric polychlorinated biphenyls (PCBs), organochlorine (OC) pesticides and polycyclic aromatic hydrocarbons (PAHs) in the Canadian Arctic: results from a decade of monitoring. Sci Total Environ 342:119–144

Hung H, Kallenbornb R, Breivikb K, Sua Y, Brorström-Lundénd E et al (2010) Atmospheric monitoring of organic pollutants in the Arctic under the Arctic Monitoring and Assessment Programme (AMAP): 1993–2006. Sci Total Environ 408:2854–2873

Intergovernmental Panel on Climate Change (IPCC) (2007) Climate Change 2007: the physical science basis. In: Solomon S, Qin D, Manning M, Chen Z, Marquis M et al (eds) Contribution of Working Group I to the Fourth Assessment Report of the Intergovernmental Panel on Climate Change. Cambridge University Press, Cambridge

Jacobi H-W, Kaleschke L, Richter A, Rozanov A, Burrows JP (2006) Observation of a fast ozone loss in the marginal ice zone of the Arctic Ocean. J Geophys Res 111:D15309. doi:10.1029/2005JD006715

Jacobi HW, Morin S, Bottenheim JW (2010) Observation of widespread depletion of ozone in the springtime boundary layer of the central Arctic linked to mesoscale synoptic conditions. J Geophys Res 115:D17302. doi:10.1029/2010JD013940

Johannessen OM, Bengtsson L, Miles MW, Kuzmina SI, Semenov VA et al (2004) Arctic climate change-observed and modelled temperature and sea ice. Tellus Ser A 56:328–341

Kaleschke L, Richter A, Burrows J, Afe O, Heygster G et al (2004) Frost flowers on sea ice as a source of sea salt and their influence on tropospheric halogen chemistry. Geophys Res Lett 31:L16114. doi:10.1029/2004GL020655

Kirk JL, St Louis VL, Sharp MJ (2006) Rapid reduction and reemission of mercury deposited into snow packs during atmospheric mercury depletion events at Churchill, Manitoba, Canada. Environ Sci Technol 40:7590–7596

Knepp TN, Bottenheim J, Carlsen M, Carlson D, Donohoue D (2010) Development of an autonomous sea ice tethered buoy for the study of ocean–atmosphere-sea ice-snow pack interactions: the O-buoy. Atmos Meas Tech 3:249–261. doi:10.5194/amt-3-249-2010

Lalonde JD, Doyon MR, Auclair JC (2003) Photo-induced Hg(II) reduction in snow from the remote and temperate Experimental Lakes Area (Ontario, Canada). J Geophys Res 108(D6):4200. doi:10.1029/2001JD001534

Laprise R, Caya D, Frigon A, Paquin D (2003) Current and perturbed climate as simulated by the second-generation Canadian Regional Climate Model (CRCM-II) over northwestern North America. Clim Dyn 21:405–421

Lesins G, Duck TJ, Drummond JR (2010) Climate trends at Eureka in the Canadian High Arctic. Atmosphere–Ocean 48(2):59–80. doi:10.3137/AO1103.2010

Long Z, Perrie W, Tang CL, Dunlap E, Wang J (2011; in press) Simulated interannual variations of freshwater content and sea surface height in the Beaufort Sea. J Climate doi:10.1175/2011JCLI4121.1

Loseto LL, Lean DRS, Siciliano SD (2004) Snowmelt sources of methylmercury to High Arctic ecosystems. Environ Sci Technol 38:3004–3010. doi:0.1021/es035146n

Lu JY, Schroeder WH, Barrie LA, Steffen A, Welch HE, Martin K et al (2001) Magnification of atmospheric mercury deposition to polar regions in springtime: the link to tropospheric ozone depletion chemistry. Geophys Res Lett 28:3219–3222

Lüers J, Bareiss J (2010) The effect of misleading surface temperature estimations on the sensible heat fluxes at a high Arctic site—the Arctic Turbulence Experiment 2006 on Svalbard (ARCTEX-2006). Atmos Chem Phys 10:157–168

Ma J, Cao Z (2010) Quantifying the perturbations of persistent organic pollutants induced by climate change. Environ Sci Technol 44:8567–8573

Ma J, Hung H, Tian C, Kallenborn R (2011) Revolatilization of persistent organic pollutants in the Arctic induced by climate change. Nature Clim Change 1:255–260

Macdonald RW, Barrie LA, Bidleman TF, Diamond ML, Gregor RG et al (2000) Contaminants in the Canadian Arctic: 5 years of progress in understanding sources occurrence and pathways. Sci Total Environ 254:93–234

Manson AH, Meek CE, Chshyolkova T, Xu X, Aso T et al (2009) Arctic tidal characteristics at Eureka (80 °N, 86 °W) and Svalbard (78 °N, 16 °E) for 2006/7: seasonal and longitudinal variations, migrating and non-migrating tides. Ann Geophys 27:1153–1173

Maslanik JA, Fowler C, Stroeve J, Drobot S, Zwally J et al (2007) A younger, thinner Arctic ice cover: increase potential for rapid, extensive sea-ice loss. Geophys Res Lett 34(24):L24501. doi:10.1029/2007GL032043

McElroy CT, McLinden CA, McConnell JC (1999) Evidence for bromine monoxide in the free troposphere during the Arctic polar sunrise. Nature 397:338–341

Melling et al (2011) this issue

Mellor GL, Kantha LH (1989) An ice-ocean coupled model. J Geophys Res 94:10937–10954

Mitchell CPJ, Branfireun BA, Kolka RK (2008) Assessing sulfate and carbon controls on net methylmercury production in peatlands: an in situ mesocosm approach. Appl Geochem 23:503–518. doi:10.1016/j.apgeochem.2007.12.020

Morey SL, Baig S, Bourassa MA, Dukhovskoy DS, O'Brien JJ (2006) Remote forcing contribution to storm-induced sea level rise during Hurricane Dennis. Geophys Res Lett 33:L19603. doi:10.1029/2006GL027021

Morin S, Hönninger G, Staebler RM, Bottenheim JW (2005) A high time resolution study of boundary layer ozone chemistry and dynamics over the Arctic Ocean near Alert. Nunavut Geophys Res Lett 32:L08809. doi:10.1029/2004GL022098

Mulligan RP, Perrie W, Solomon S (2010) Dynamics of the Mackenzie River plume on the inner Beaufort shelf during an open water period in summer. Estuar Coast Shelf Sci 89:214–220. doi:10.1016/j.ecss.2010.06.010

Natural Environment research Council (NERC) (2009) [Carpenter LJ, Ball S, Coe H, Evans MJ, Gallagher MWG et al]. Impact of combined iodine and bromine release on the Arctic atmosphere (COBRA), [Internet]. NCAS British Atmospheric Data Centre, Date of citation. Available from http://badc.nerc.ac.uk/view/badc.nerc.ac.uk__ATOM__dataent_12330719779627095

Nghiem SV, Rigor IG, Perovich DK, Clemente-Colón P, Weatherly JW et al (2007) Rapid reduction of Arctic perennial sea ice. Geophys Res Lett 34:L19504. doi:10.1029/2007GL031138

Oltmans S, Komhyr W (1986) Surface ozone distributions and variations from 1973 to 1984 measurements at the NOAA Geophysical Monitoring for Climatic Change Baseline Observatories. J Geophys Res 91:D4. doi:10.1029/JD091iD04p05229

O'Neill NT, Perro C, Saha A, Lesin G, Duck T et al (2011; submitted) Impact of Sarychev sulphate aerosols over the Arctic. J Geophys Res

Perrie W, Ren X, Zhang W, Long Z (2004) Simulation of extratropical Hurricane Gustav using a coupled atmosphere–ocean-sea spray model. Geophys Res Lett 31:L03110. doi:10.1029/2003GL018571

Piot M, von Glasow R (2008) The potential importance of frost flowers, recycling on snow, and open leads for ozone depletion events. Atmos Chem Phys 8:2437–2467

Pisaric MFJ, Thienpont JR, Kokelj SV, Nesbitt H, Lantz TC et al (2011) Impacts of a recent storm surge on an Arctic delta ecosystem examined in the context of the last millennium. Proc National Acad Sci. doi/10.1073/pnas.1018527108

Pöhler D, Vogel L, Friess U, Platt U (2010) Observation of halogen species in the Amundsen Gulf, Arctic, by active long-path differential optical absorption spectroscopy. Proc Nat Acad Science 107:6582–6587

Poulain AJ, Lalonde JD, Amyot M, Shead JA, Raofie F et al (2004) Redox transformations of mercury in an Arctic snowpack at springtime. Atmos Environ 38:6763–6774

Rahn KA, Heidam NZ (1981) Progress in Arctic air chemistry 1977–1980: a comparison of the first and second symposium. Atmos Environ 15:1345–1348

Richter A, Wittrock F, Eisinger M, Burrows JP (1998) GOME observations of tropospheric BrO in northern hemispheric spring and summer 1997. Geophys Res Lett 25(14):2683–2686

Richter A, Wittrock F, Ladstätter-Weissenmayer A, Burrows JP (2002) GOME measurements of stratospheric and tropospheric BrO. Adv Space Res 29:1667–1672

Ridley BA, Zeng T, Wang Y, Atlas EL, Browell EV et al (2007) An ozone depletion event in the sub-arctic surface layer over Hudson Bay, Canada. J Atmos Chem 57:255–280

Saha A, O'Neill NT, Eloranta E, Stone RS, Eck TF et al (2010) Pan-Arctic sunphotometry during the ARCTAS-A campaign of April 2008. Geophys Res Lett 37:L05803. doi:10.1029/2009GL041375

Saha A, O'Neill NT, Stone RS, Liu P, Herber A (2011; submitted) Analysis of sub-micron parameters derived from multi-altitude and multi-spectral AOD measurements acquired during the 2009 PAM-ARCMIP airborne campaign. IPY Special Issue of Atmospheric Environment

Salawitch RJ, Canty T, Kurosu T, Chance K, Liang Q (2010) A new interpretation of total column BrO during Arctic spring. Geophys Res Lett 37:L21805

Schade LR, Emanuel KA (1999) The ocean's effect on the intensity of tropical cyclones: results from a simple coupled atmosphere–ocean model. J Atmos Sci 56:642–651

Schroeder WH, Anlauf KG, Barrie LA, Lu JY, Steffen A et al (1998) Arctic springtime depletion of mercury. Nature 394:331–332

Seabrook JA, Whiteway J, Staebler RM, Bottenheim JW, Komguem L et al (2011) LIDAR measurements of Arctic boundary layer ozone depletion events over the frozen Arctic Ocean. J Geophys Res 116:D00S02. doi:10.1029/2011JD016335

Serreze MC, Lynch AH, Clark MP (2001) The Arctic frontal zone as seen in the NCEP-NCAR reanalysis. J Clim 14:1550–1567

Serreze MC, Holland MM, Stroeve J (2007) Perspectives on the Arctic's shrinking sea-ice cover. Science 315:1533–1536. doi:10.1126/science.1139426

Simmonds I, Burke C, Keay K (2008) Arctic climate change as manifest in cyclone behavior. J Climate 21:5777–5796. doi:10.1175/2008JCLI2366.1

Simmonds I, Keay K (2009) Extraordinary September Arctic sea ice reductions and their relationships with storm behavior over 1979–2008. Geophys Res Lett 36:L19715. doi:10.1029/2009GL039810

Simpson WR, von Glasow R, Riedel K, Anderson P, Ariya P et al (2007a) Halogens and their role in polar boundary-layer ozone depletion. Atmos Chem Phys 7:4375–4418

Simpson WR, Carlson D, Hönninger G, Douglas TA, Sturm M (2007b) First-year sea-ice contact predicts bromine monoxide (BrO) levels at Barrow, Alaska better than potential frost flower contact. Atmos Chem Phys 7:621–627

Small D, Atallah E, Gyakum J (2011) Wind regimes along the Beaufort Sea coast favorable for strong wind events at Tuktoyaktuk. J Appl Meteorol Climatol 50:291–1306. doi:10.1175/2010JAMC2606.1

Sodemann H, Foken T (2005) Special characteristics of the temperature structure near the surface. Theor Appl Climatol 80:81–89

Solomon S (1994) Monitoring coastal change along the Canadian Beaufort Sea: report on the field activities. Geological Survey of Canada, Open File No. 3009, p 23

Steele M, Morley R, Ermold W (2001) PHC: A global ocean hydrography with a high-quality Arctic Ocean. J Climate 14:2079–2087

Steffen A, Schroeder WH, Bottenheim J, Narayan J, Fuentes JD (2002) Atmospheric mercury concentrations: measurements and profiles near snow and ice surfaces in the Canadian Arctic during Alert 2000. Atmos Environ 36:2653–2661

Steffen A, Douglas T, Amyot M, Ariya P, Aspmo K et al (2008) A synthesis of atmospheric mercury depletion event chemistry in the atmosphere and snow. Atmos Chem Phys 8:1445–1482. doi:10.5194/acp-8-1445-2008

Sunderland EM, Krabbenhoft DP, Moreau JW, Strode SA, Landing WM (2009) Mercury sources, distribution, and bioavailability in the North Pacific Ocean: insights from data and models. Global Biogeochem Cycles 23:GB2010. doi:10.1029/2008GB003425

Wagner T, Platt U (1998) Satellite mapping of enhanced BrO concentrations in the troposphere. Nature 395 (486–490)

Weiss-Penzia P, Jaffe D, Mcclintick A, Prestbo E, Landis M (2003) Gaseous elemental mercury in the marine boundary layer: evidence for rapid removal in anthropogenic pollution. Environ Sci Technol 37:3755–3763

Wong F, Jantunen LM, Puko M, Papakyriakou T, Staebler RM et al (2011) Air-water exchange of anthropogenic and natural organohalogens on International Polar Year (IPY) Expeditions in the Canadian Arctic. Environ Sci Technol 45:876–881

Yagüe C, Maqueda G, Rees JM (2001) Characteristics of turbulence in the lower atmosphere at Halley IV Station, Antartica. Dyn Atmos Oceans 34:205–223

Xu X, Manson AH, Meek CE, Chshyolkova T, Drummond JR et al (2009a) Vertical and inter-hemispheric links in the stratosphere-mesosphere as revealed by the day-to-day variability of Aura-MLS temperature data. Ann Geophys 27:3387–3409

Xu X, Manson AH, Meek CE, Chshyolkova T, Drummond JR et al (2009b) Relationship between variability of the semidiurnal tide in the Northern Hemisphere mesosphere and quasi-stationary planetary waves throughout the global middle atmosphere. Ann Geophys 27:4239–4256

Zhang X, Walsh JE, Zhang J, Bhatt US, Ikeda M (2004) Climatology and interannual variability of Arctic cyclone activity: 1948–2002. J Climate 17:2300–2317